Langmuir-Blodgett film formation and second-harmonic generation of poly(isocyanide)s

Teerenstra, Marcel Nicolaas

Chapter 4

A study of the structure of mono- and multilayers of poly(isocyanide)s with NLO-active side chains by infrared, ellipsometry, and electron microscopy

Summary

The properties and structure of Langmuir-Blodgett mono- and multilayers of several poly(isocyanide)s with NLO-active side chains are reported. These polymers form very rigid layers or layers which appear to be unstable. To circumvent this problem the polymers are mixed with other poly(isocyanide)s and with amylose butyrate. Transmission electron microscopy studies of the polymeric mixtures reveal that phase separation occurs in all cases and that only poly(isocyanide)s substituted with hydrophilic side chains form monomolecular layers. Depending on the nature of the polymer which is used for mixing, Y- or Z-type LB films can be obtained. In the LB films the side chains of the polymers are oriented more or less perpendicular to the film plane, unless these side chains are large, in which case they adopt a more parallel orientation.

Introduction

The Langmuir-Blodgett (LB) technique offers the possibility to organize molecules into highly ordered monolayers and to produce multilayer films with desired architectures. Owing to stronger intra- and intermolecular interactions, polymeric LB films tend to have better thermal and mechanical stability than those of low molecular weight compounds. In spite of the fact that in some cases, polymeric Langmuir-Blodgett films have a lower degree of order they are expected to have great potential for applications in the field of sensors, optonics, and electronics.

Many polymers have already been used to form monolayers at the air-water interface. They can roughly be devided in two classes: comb-like polymers which resemble low

molecular weight amphiphiles [1-8] and rigid-rod polymers [9-14]. Recently, a number of studies have appeared dealing with polymeric nonlinear optical (NLO) materials. Non-linear optically active moieties have been incorporated in polymer matrices as low molecular weight compounds [15,16,17] or have been introduced in the backbone [18,19] or side groups [20-23] of polymers.

In this Chapter poly(isocyanide)s, $[R\text{-}N{=}C{<}]_n$, are investigated with pendent NLO-active substituents. These polymers have a very stable helical conformation. A tightly coiled 4_1-helical backbone is formed during polymerization [24]. Polymerization of one enantiomer of a chiral isocyanide gives rise to the formation of polymer helices with an excess of one particular screw sense. Since a helix is a chiral species, this should lead to non-centro-symmetric structures. Attaching NLO-active groups to these helices might result in polymers which can exhibit second-harmonic generation (SHG).

Experimental

Synthesis

The route which was used to synthesize the different polymers is given in Scheme 4.1. The general procedures have been outlined in the experimental section of Chapter 2. Together with Table 4.1, Scheme 4.1 shows which precursors and polymers were synthesized and investigated in this Chapter. The polymeric structures and their codes are listed in Appendix 1. A detailed description of the synthesis of the compounds is given in Appendix 2.

Scheme 4.1

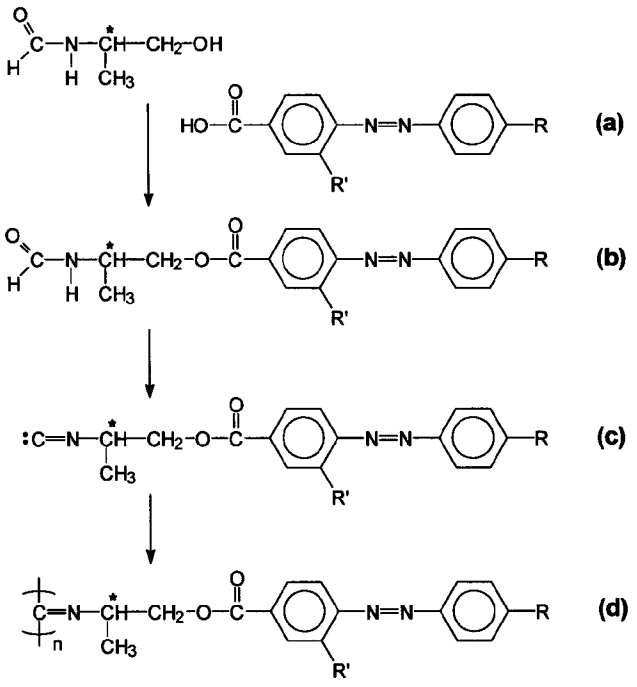

Table 4.1: *Polymers and their precursors used in this study.*[a]

Compound	R	R'	Configuration at C*
7 a,b,c,d	$N(CH_3)_2$	H	(R,S)
8 a,b,c,d	$N(n\text{-}C_4H_9)_2$	H	(R,S)
9 a,b,c,d	$N(n\text{-}C_4H_9)_2$	H	(S)
10 a,b,c,d	$N(n\text{-}C_4H_9)_2$	NO_2	(S)
11 a,b,c,d	$N(C_2H_4OC(O)CH_3)_2$	NO_2	(S)
12 a,b,c,d	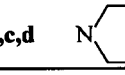	NO_2	(R,S)

[a] *For structures see Scheme 4.1.*

Ellipsometry

Film thicknesses were measured using a Gaertner L117-c or L117 Production Ellipsometer at a wavelength of 632.8 nm as well as with a home-built spectrometer. The latter was an automated four-zone ellipsometer [25] with a spectral range between 214 and 2300 nm and a resolution of 0.01 nm (typically chosen at 1 nm). The measured parameters Δ and Ψ had a relative accuracy of $2 \cdot 10^{-4}$ degrees and an absolute reproducibility of 10^{-3} degrees. Refractive indices of the multilayered films were determined at chosen wavelengths (typically 532, 632.8 and 1064 nm).

Spectral simulations

IR spectra of thin films deposited on different substrates generally are modified by optical effects. Distinguishing the changes observed in the spectra caused by these effects is crucial for the interpretation of the spectroscopic data and must be done before relating any differences in band shape, position, and intensity to structural, orientational and/or chemical bonding changes in the film. Therefore, spectral simulations has been used to elucidate the influence of these optical effects and to make comparison of the various spectra possible [26,27].

The optical constants of the polymers, necessary for the spectral simulations were calculated according to the following procedure. A transmission spectrum of a free standing film of the polymer was used as an input spectrum. The thickness of this film and the refractive index, n, were calculated using ellipsometric data obtained from measurements of LB films on silicon. The absorption coefficients were converted into wave vector (k) values after which the refractive index (n) spectrum could be calculated from the estimated k-spectrum with the Kramers-Kronig relationship [26]. For the optical constants of the ZnS and gold substrates the refractive indices 2.22 and $9.5\text{-}30i$ were used, respectively [28].

Results and discussion

Monolayer behaviour and transfer of poly(isocyanide)s with hydrophobic side chains

Poly(isocyanide) **5** (Table 2.1) forms stable, Z-type transferable monolayers, probably due to the fact that its side chains are hydrophilic and interact strongly and cooperatively with the water subphase [14]. Substitution of the ester function of **5** by large hydrophobic groups results in polymers **7, 8, 9**, and **10**. Polymer **7** was found to be insoluble in common solvents and could only be spread from a mixture of methanesulfonic acid and chloroform. Polymers **8**, **9**, and **10**, however, are soluble in chloroform but they did not form stable monolayers, probably because of lack of interaction of the side chains with the water subphase. However, upon mixing them with amylose ester derivatives *i.e.* amylose acetate or amylose butyrate (**AB**), stable and transferable films were formed.

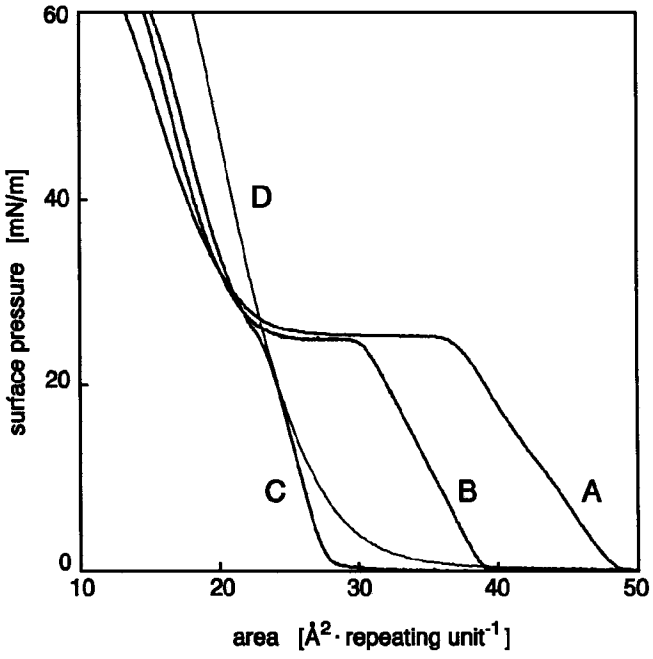

Figure 4.1: *Pressure-area isotherms of mixtures of **10** and **AB**. The mole fraction of **10** is 0.00 (A, pure **AB**), 0.28 (B), 0.66 (C) and 1.00 (D, pure **10**). T = 15°C.*

Isotherms of films of **AB** mixed with increasing concentrations of poly(isocyanide)s **8** and **10**, showed a decreasing area A_0, which is the area found by extrapolating the linear increase in the pressure-area isotherm to π=0 mN/m (Figure 4.1). Moreover, in the entire range A_0 was smaller than the value given by the additivity rule (4.1)

$$A_{0,mixture} = f_{polymer} * A_{0,polymer} + (1-f_{polymer}) * A_{0,AB} \qquad (4.1)$$

in which $f_{polymer}$, $A_{0,polymer}$, and $A_{0,AB}$ denote the mole fraction of the poly(isocyanide)s the specific area of the poly(isocyanide), and the specific area of the amylose butyrate, respectively. Figure 4.2 shows the area A_0 of **8** and **10** as a function of the mole fraction of these polymers in mixtures with **AB**.

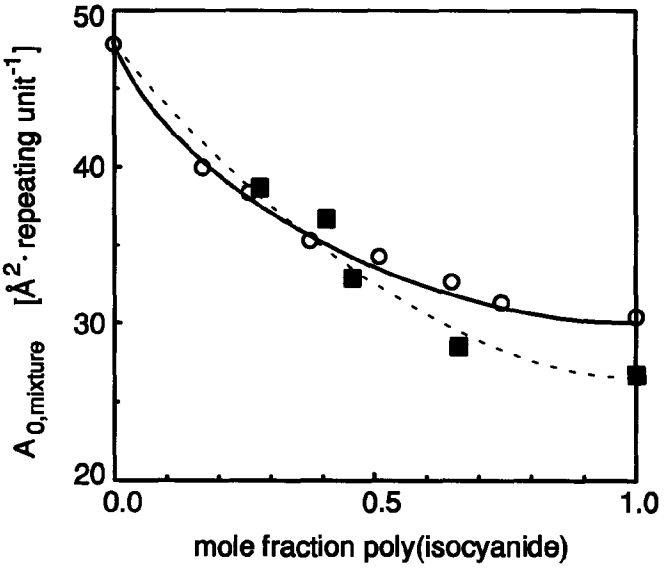

Figure 4.2: *The specific area $A_{0,mixture}$ of **8** (○) and **10** (■), as a function of the mole fraction of these polymers in mixtures with **AB**.*

Pure **AB** is known to form well defined, stable monolayers in which the polymer molecules have a helical conformation [29]. Monolayers of **AB** could be deposited on solid substrates with transfer ratios of 0.7 during the downstroke run and 1.0 during the upstroke run. Given this fact it is likely that in the mixtures with **8** and **10** the amylose butyrate is completely situated at the air-water interface. From the negative deviation in Figure 4.2 it can be concluded that for the poly(isocyanide)s molecules less room will be available at this interface. Figure 4.3 shows the effect of **AB** on the stability of the monolayers. As can be seen the area per repeating unit for pure **10** decreases as a function of time even after one hour, in contrast to the layers containing **AB**, which are stable. Unlike the films of the pure poly(isocyanide)s the mixed films could be transferred easily. At least 100 successive layers could be deposited (Y-type) with transfer ratios of 0.75 during downstroke dipping and 1.00 during upstroke dipping. Monolayer thicknesses were calculated from ellipsometrical measurements on deposited multilayers. For these experiments silicon substrates were covered with 16, 32, 48, 64, 80, and 96 successive monolayers, respectively, prepared from mixed films of **10** and **AB**. As can be seen in Table 4.2 the monolayer thickness depends on the mole fraction of **10**. Extrapolation of the values yields a monolayer thickness, d_0, of 27.3 Å for pure **10**.

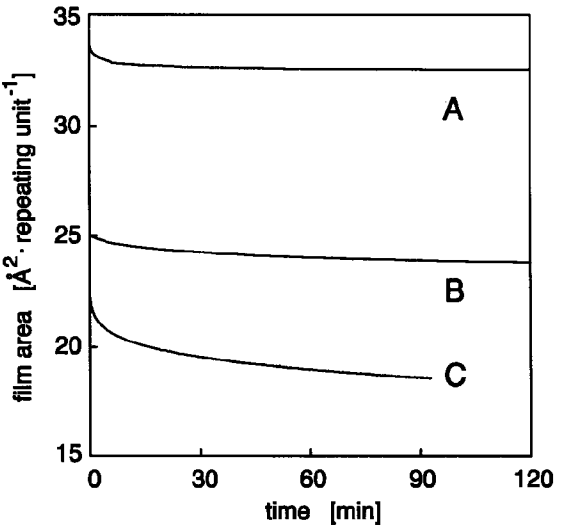

Figure 4.3: *Stabilization curves of mixtures of **10** and **AB** at a surface pressure of 15 mN/m. The mol fraction of **10** is 0.28 (A), 0.66 (B), and 1.00 (C, pure **10**). T= 17°C in all cases.*

Table 4.2: *Monolayer thicknesses of AB and mixtures of 10 with AB, measured by ellipsometry.*

Polymer	Mole fraction poly(isocyanide)	d_0 (nm)
AB	0.00	1.11
	0.28	1.52
	0.46	1.85
	0.66	2.18
10	1.00	2.73 [a]

[a] *extrapolated value.*

Transmission electron microscopy (TEM) pictures of the mixed films taken from the water-side show separate domains of **10** and **AB**. Pure **10** (Figure 4.4A) forms a layer which is smooth over large areas but which also contains thicker domains. These domains are visible as dark circular patches with a cross section of about 250 nm. The wrinkles seen on the micrograph are probably caused by collapse of the layer. Figure 4.4B shows a mixed film of 66% **10** in **AB**. The **AB** domains have a bumpy surface. The poly(isocyanide) forms irregularly shaped domains of about 1 μm and the thick areas of this polymer are still present. The surfaces of the thin areas of **10** are higher than the **AB** domains, as can be seen at the boundary lines of the different phases. The collapse wrinkles are not as pronounced as in the films of pure **10**. In the mixed film, consisting of 28% **10** (Figure 4.4C), the domains of **10** have become smaller (<100 nm). Moreover, the collapse is completely suppressed.

The mixed films were also observed from the air-side. Figure 4.4D shows such a film composed of 28% **10** in **AB**. The **AB** matrix gives the impression of being rather smooth. The dark domains of **10** are only slightly higher than the domains of **AB**. From the foregoing results we may conclude that mixed films of **10** and **AB** can be represented schematically as depicted in Figure 4.5. Polymer **10** is present as lenticular domains which are thinned out to a monolayer thickness at their edges. The **AB** phase is clearly asymmetric, being rough at the water-side and very smooth at the air-side of the layer. Only minor height differences are observed.

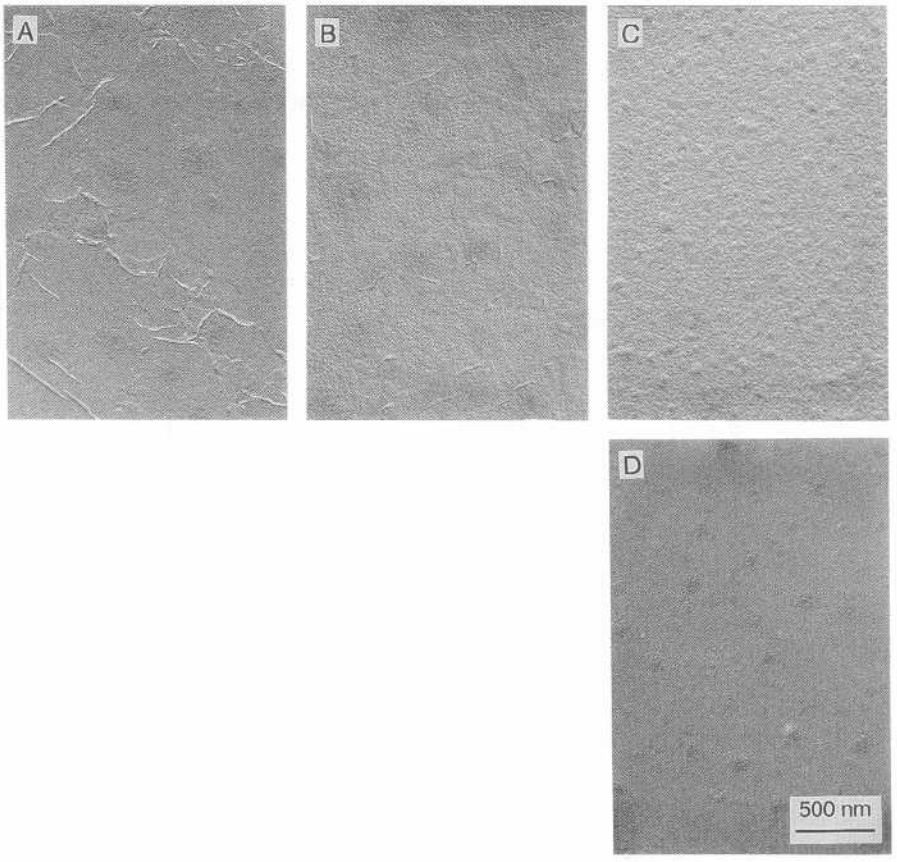

Figure 4.4: *TEM micrographs with view on the water-side: pure **10** (A), 66% **10** in **AB** (B), and 28% **10** in **AB** (C). Idem with view on the air-side: 28% **10** in **AB** (D).*

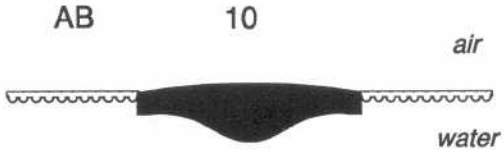

Figure 4.5: *Schematic representation of a mixed layer of polymer **10** and **AB**.*

Monolayer behaviour and transfer of poly(isocyanide)s with hydrophilic side chains

The pressure-area isotherms of polymer **12** and mixtures of polymer **12** with polymer **5** showed a gradual increase of the surface pressure when the surface area was reduced (Figure 4.6).

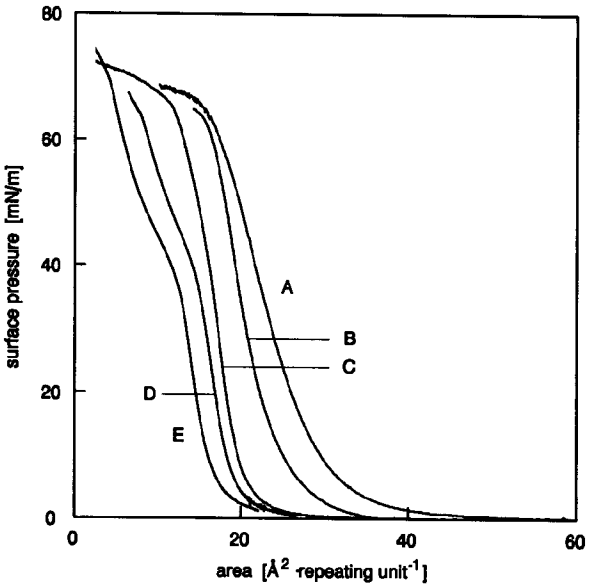

Figure 4.6: *Pressure-area isotherms at 15°C of mixtures of polymer **12** and polymer **5**. The mole fractions of **12** are 1.00 (pure **12** ,A), 0.69 (B), 0.45 (C), 0.15 (D), and 0.00 (pure **5**, E), respectively.*

Over the entire range of compositions, $A_{0,mixture}$ corresponded to the value given by the additivity rule (Equation 4.1). Figure 4.7 shows $A_{0,mixturre}$ of **11** and **12** as a function of the mole fraction of these polymers in mixtures with **5**.

Poly(isocyanide)s **11** and **12**, which have hydrophilic side chains formed, stable monomolecular layers without the requirement of mixing these polymers with **AB**. The obtained films were, however, very rigid and as a consequence could not be transferred with the conventional vertical dipping method. When polymers **11** and **12** were mixed

with **5**, the stability of the films remained the same but vertical transfer of the monolayers became possible by Z-type deposition for at least 100 successive dippings. The transfer ratios and film stabilities were not affected up to a mole fraction of 0.6 of poly(isocyanide) **12** in the mixture with **5**. In contrast to what was described in Chapter 4, the mixtures of **11** and **12** with **5** showed areas A_0 which followed Equation 4.1 (Figure 4.7). Due to their more hydrophilic side chains poly(isocyanide)s **11** and **12** have the possibility to be located at the water surface. They can form hydrogen bonds with the water subphase more easily than polymers **8**, **9**, and **10**. In the TEM micrograph of a film of a mixture of 37% **12** in **5** (Figure 4.8) separate domains of the two polymers are visible. It is clear that the dark lens-shaped domains, present in the mixtures of **10** and **AB** (Figure 4.4), do not show up here. A smooth monolayer with only minor height differences is observed.

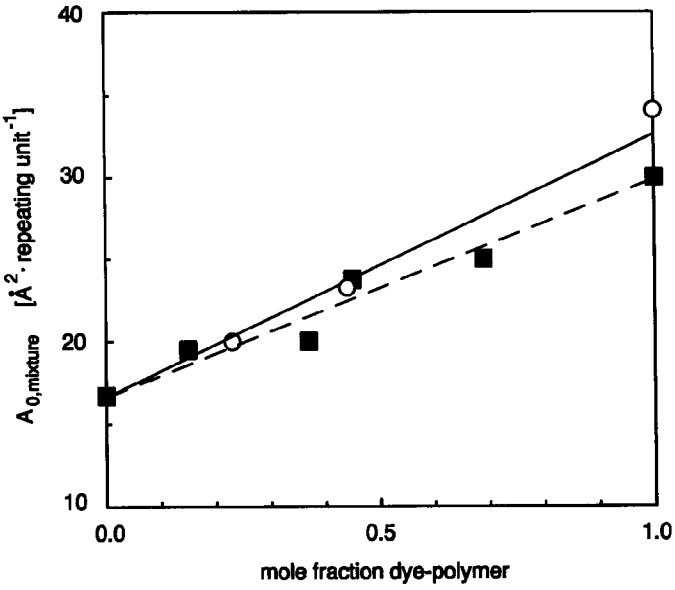

Figure 4.7: *Specific area, $A_{0,mixture}$, of polymers **11** (○) and **12** (■) derived from pressure-area isotherms of mixtures with **5**.*

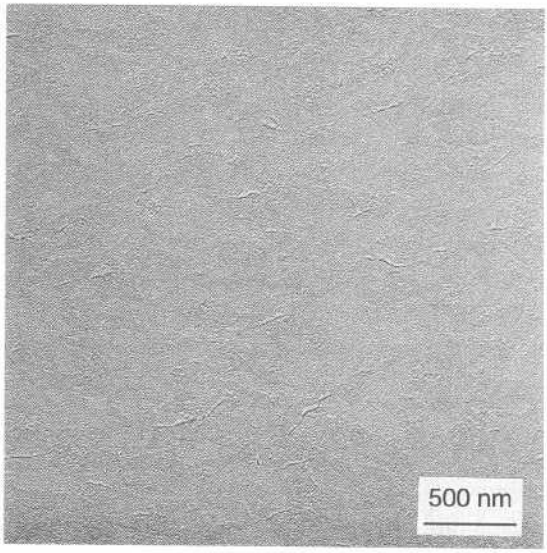

Figure 4.8: *Transmission electron micrograph of a mixed monolayer of polymer* ***12*** *and* ***5*** *(37 mole%* ***12*** *in* ***5****).*

Infrared spectroscopy

The LB films of polymers **11** and **12** and those of mixtures of these polymers with **5** were studied by transmission and grazing incidence IR spectroscopy. Spectral simulations were carried out to obtain information about possible orientational effects in the films. Transmission spectra with different polarizations of the IR light revealed that in the case of a mixture of 44 mole% **11** in **5**, the latter polymer was oriented in the same way as found in Chapter 2, *i.e.* with its helical axis parallel to the transfer direction. For polymers **11** and **12** we can expect that the flow induced orientation of the molecules is small because the polymers have a low degree of polymerization ($P_n \approx 100$ for both polymers) and a large side chain, leading to an aspect ratio of only 2.5.

In order to study the orientation of the polymer side chains, mixed LB films of polymers **11** and **12** with polymer **5**, were prepared. In the case of polymer **11** the mixture contained 44 mole% of this polymer. The sample used in the transmission experiments was composed of 20 layers which were deposited on both sides of a ZnS substrate and had a total thickness of 77.6 nm. For the calculation of the spectrum the refractive index

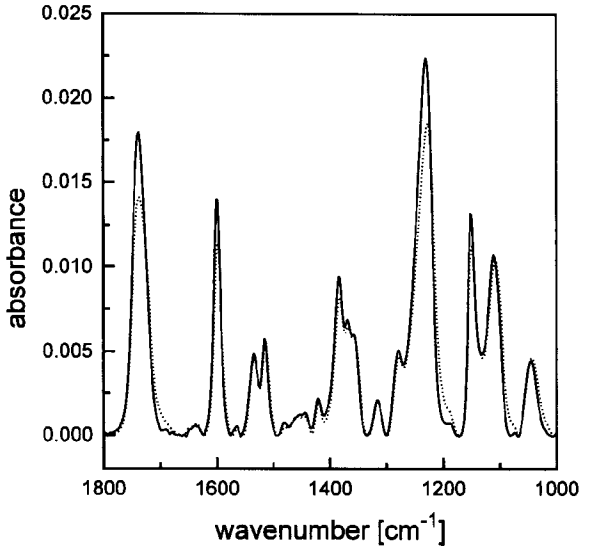

Figure 4.9a: *Transmission IR spectra of a mixed LB film of polymer 11 and 5 (44 mole% 11). Calculated (.....) and experimental (———) spectrum.*

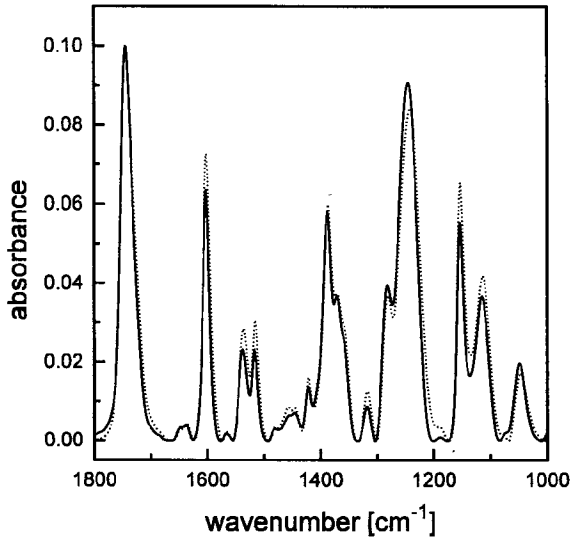

Figure 4.9b: *Grazing incidence reflection IR spectra of a mixed LB film of polymer 11 and 5 (44 mole% 11). Calculated (.....) and experimental (———) spectrum.*

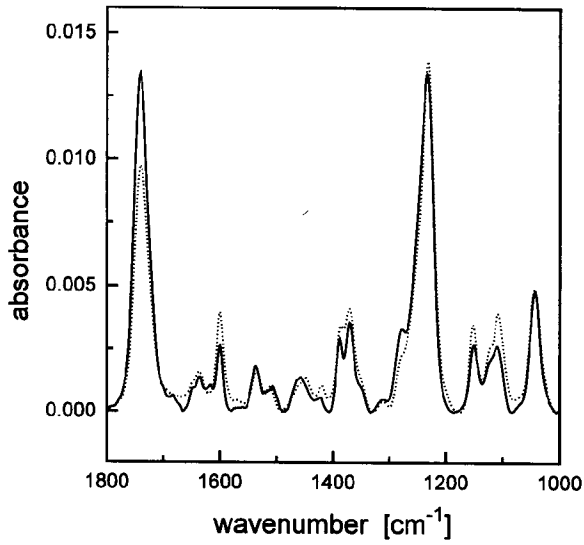

Figure 4.10a: *Transmission IR spectra of a mixed LB film of polymer* ***12*** *and* ***5*** *(15 mole% 12). Calculated (.....) and experimental (———) spectrum.*

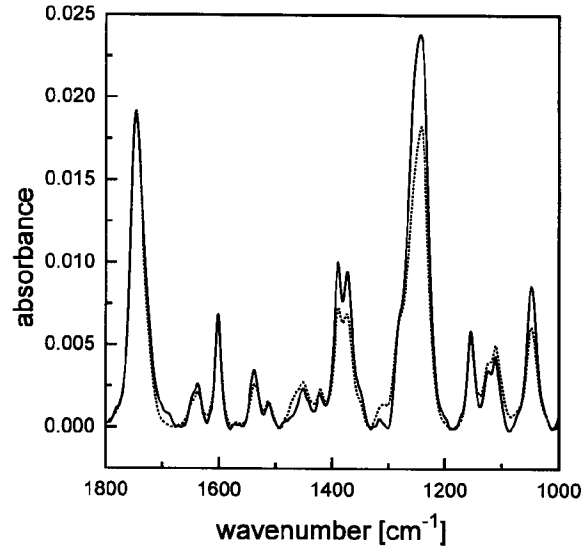

Figure 4.10b: *Grazing incidence reflection IR spectra of a mixed LB film of polymer* ***12*** *and* ***5*** *(15 mole% 12). Calculated (.....) and experimental (———) spectrum.*

was assumed to be 1.50. The sample used in the GIR experiments contained 31 layers with a total layer thickness of 60 nm. The experimental transmission spectra showed only minor deviations from the calculated spectrum. The absorption peak at 1600 cm^{-1}, originating from the bending vibration of the aromatic rings, was found to be larger compared to this absorption in the calculated spectrum suggesting that the chromophoric groups had a orientation which is predominantly parallel with respect to the film (Figure 4.9a). In case of the GIR spectrum the experimentally determined absorption at 1600 cm^{-1} was lower then the calculated one (Figure 4.9b). This points to an orientation of the chromophoric groups which is slightly parallel to the plane of the film.
The mixed film of polymer **12** and **5** contained 15 mole% of the former component. The sample used in the transmission experiments had 20 layers covering both sides of the substrate ZnS. Its total thickness was 56.4 nm. The refractive index used in the calculation of the spectrum was 1.45. The GIR sample contained 12 layers with a total layer thickness of 16.9 nm. The transmission spectra (without polarization of the IR light) showed a lower absorption at 1600 cm^{-1} than the simulated spectra (Figure 4.10a). This indicates that the chromophoric groups must be oriented predominantly perpendicular to the substrate. The coinciding absorption peaks at 1600 cm^{-1} in the experimental and calculated GIR spectra (Figure 4.10b) indicate, however, that the side groups have an orientation which is random. These observations together with the results obtained from ellipsometric measurements, to be discussed in the next section, allow us to propose a model of the conformation of the side chains of the two polymers in the LB films.

Ellipsometry

The thicknesses of the LB multilayers were determined ellipsometrically, using a wavelength of 632.8 nm. In order to be able to calculate the linear and non-linear Fresnel factors we also measured the refractive indices at wavelengths of 532 nm ($n_{2\omega}$) and 1064 nm (n_{ω}).
Different mixtures of polymers **11** and **12** with polymer **5** were used. They were deposited on a silicon substrate and consisted of 16 up to 80 successive monolayers per sample. The monolayer thickness, was calculated by extrapolating the measured thickness to a composition of pure polymer **11** or **12**. The results appeared to be quite different for the two polymers. (Table 4.3)

Table: 4.3: *Refractive indices at 1064 nm (n_ω) and 532 nm ($n_{2\omega}$), and average monolayer thicknesses of mixed monolayers of polymers 11 and 12 with polymer 5.*

Polymer	Mole fraction of dye-polymer	n_ω	$n_{2\omega}$	d_0 (nm)
5	-	1.45	1.50	1.32
11	0.23	1.56	1.83	1.81
	0.44	1.53	1.90	1.94
	1.00			2.81 [a]
12	0.15	1.55	1.60	1.41
	0.56	1.62	1.78	1.63
	1.00			1.88 [a]

[a] *These monolayer thicknesses were determined by extrapolation.*

From molecular models it can be calculated that polymer **12** has a maximum cross section of approximately 39 Å, which is 5 Å less than that of polymer **11**, *viz.* 44 Å. The more compact structure of the morpholine group in **12** compared to the di-esteramino group in **11** may therefore be responsible for the observed smaller film thickness. Another reason may be that the ester functions present in polymer **11** repel each other, causing the film to be thicker. This would be in agreement with the infrared measurements, which showed that the side chains of polymer **12** adopt a more parallel orientation with respect to each other. Due to the bulkier ester groups in **11** such a side chains packing is not possible for this polymer.

In Figure 4.11 we show possible conformations for the side groups of polymer **11** and **12** which are in agreement with the results obtained from the infrared and ellipsometric measurements. The cross section of polymer **11** is depicted larger than that of polymer **12**. This is in agreement with the slightly larger areas per repeating unit found in the pressure-area isotherms of the former polymer (Figure 4.7) and also in agreement with the fact that the monolayer of this polymer is thicker. In case of polymer **12** the average orientation of the chromophoric side groups is somewhat more perpendicular to the film plane than in the case of polymer **11**. It should be noted however that, this average orientation of the side chains is only slightly deviating from a random alignment.

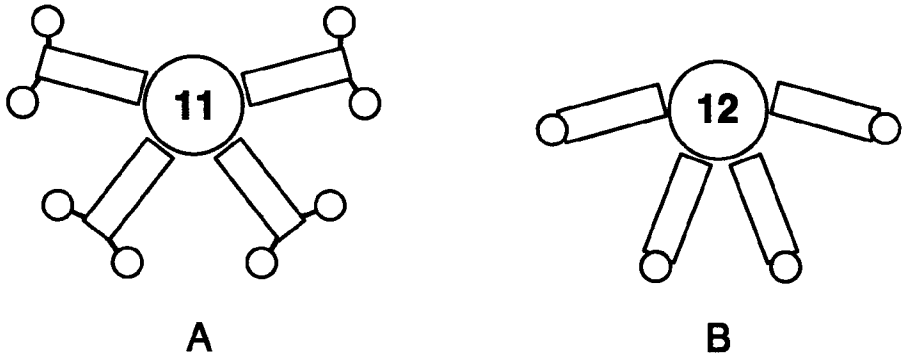

Figure 4.11: *Schematic representation of the conformation of the side chains of polymers 11 (A) and 12 (B) in the LB film. One helical turn is shown.*

Conclusions

The poly(isocyanide)s described in this Chapter form very rigid monolayers. When they are mixed with amylose butyrate or with polymer **5** in transferable films. In these mixed films the poly(isocyanide)s with relatively hydrophobic side chains are partly present as thick domains. Transfer ratios appear to remain constant, even after 100 depositions and clear films with thicknesses of over 0.3 μm can be obtained. The poly(isocyanide)s with hydrophilic side chains also form rigid monolayers but in contrast to the polymers with the hydrophobic side chains they are located at the air-water interface. The side chains of these hydrophilic polymers are slightly oriented. When these side chains are small they are oriented more perpendicular to the substrate than when they are large.

References

1 T. Kawaguchi, N. Nakahara and K. Fukuda, *J. Colloid Interface Sci.*, **104** (1985) 290.
2 T.L. Penner, J.S. Schildkraut, H. Ringsdorf and A. Schuster, *Macromolecules*, **24** (1991) 1041.
3 J. Schneider, H. Ringsdorf and J.F. Rabolt, *Macromolecules*, **22** (1989) 205.

4 T. Seki and K. Ichimura, *Polymer Commun.*, **30** (1989) 108.
5 M.B. Biddle, J.B. Lando, H. Ringsdorf, G. Schmidt and J. Schneider, *Colloid Polym. Sci.*, **266** (1988) 806.
6 A. Laschewski, H. Ringsdorf, G. Schmidt and J. Schneider, *J. Am. Chem. Soc.*, **109** (1987) 788.
7 S.J. Mumby, J.D. Swalen and J.F. Rabolt, *Macromolecules*, **19** (1986) 1054.
8 P. Hodge, E. Khoshdel, R.H. Tredgold, A.J. Vickers and C.S. Winter, *Br. Polym. J.*, **17** (1985) 368.
9 E. Orthmann and G. Wegner, *Angew. Chem. Int. Ed. Engl.*, **25** (1986) 1105.
10 G. Wegner, *Thin Solid Films*, **216** (1992) 105.
11 C. Bubeck, D. Neher, A. Kaltbeitzel, G. Duda, T. Arndt, T. Sauer and G. Wegner, *NATO ASI Ser., Ser. E. Nonlinear Opt. Eff. Org. Polym.*, **162** (1989) 185.
12 R.G.M. Crockett, A.J. Campbell and F.R. Ahmed, *Polymer*, **31** (1990) 602.
13 G. Duda, A.J. Schouten, T. Arndt, G. Lieser, G.F. Schmidt, C. Bubeck and G. Wegner, *Thin Solid Films*, **159** (1988) 221.
14 M.N. Teerenstra, E.J. Vorenkamp, R.J.M. Nolte and A.J. Schouten, *Thin Solid Films*, **196** (1991) 153.
15 M. Eich, B. Reck, D.Y. Yoon, C.G. Willson and G. Bjorklund, *J. Appl. Phys.*, **66** (1989) 3241.
16 H.L. Hampsch, J. Yang, G.K. Wong and J.M. Torkelson, *Macromolecules*, **23** (1990) 3640.
17 G.L.J.A. Rikken, C.J.E. Seppen, S. Nijhuis and E.W. Meijer, *Appl. Phys. Lett.*, **58** (1991) 435.
18 D.J. Williams, *Thin Solid Films*, **216** (1992) 117.
19 J.D. Stenger-Smith, J.W. Fischer, R.A. Henry, J.M. Hoover, G.A. Lindsay and L.M. Hayden, *Makromol. Chem., Rappid Commun.*, **11** (1990) 141.
20 M.M. Carpenter, P.N. Prasad and A.C. Griffin, *Thin Solid Films*, **161** (1988) 315.
21 R.C. Hall, G.A. Lindsay, B. Anderson, S.T. Kowel, B.G. Higgins and P. Stroeve, *Mat. Res. Soc., Symp. Proc.*, **109** (1988) 351.
22 A.J. Vickers, R.H. Tredgold, P. Hodge, E. Khoshdel and I. Girling, *Thin Solid Films*, **134** (1985) 43.
23 T.L. Penner, N.J. Armstrong, C.S. Willand, J.S. Schildkraut and D.R. Robello, *SPIE, Nonlinear Opt. Prop. Org. Mater.*, **1560** (1991) 377.
24 W. Drenth and R.J.M. Nolte, *Acc. Chem. Res.*, **12** (1979) 30.
25 R.M.A. Azzam and N.M. Bashara, *Ellipsometry and Polarized Light*, North Holland Physics Publishing, Amsterdam, 1979.
26 R.H.G. Brinkhuis and A.J. Schouten, *Macromolecules*, **24** (1991) 1496.
27 J.A. Mielczarski, *J. Phys. Chem.*, **11** (1993) 2649.
28 D.L. Allara, A. Baca and C.A. Pryde, *Macromolecules*, **11** (1978) 1215.
29 M.A. Schoondorp, E.J. Vorenkamp and A.J. Schouten, *Thin Solid Films*, **196** (1991) 121.